

# Two-photon absorption in CdTe quantum dots

Lázaro A. Padilha<sup>1,2</sup>, Jie Fu, David J. Hagan\*, and Eric W. Van Stryland\*

<sup>1</sup>College of Optics & Photonics: CREOL & FPCE, University of Central Florida, 4000 Central Florida Blvd., 32816-2700, Orlando, FL, USA.

\*Also with the Department of Physics

[padilha@ifi.unicamp.br](mailto:padilha@ifi.unicamp.br)

Carlos L. Cesar, Luiz C. Barbosa, and Carlos H. B. Cruz

<sup>2</sup>Instituto de Física "Gleb Wataghin", Universidade Estadual de Campinas (UNICAMP), 13083-970, Campinas – SP, Brazil

**Abstract:** We report measurements of frequency degenerate and nondegenerate two-photon absorption (2PA) spectra of CdTe quantum dots, QDs, in glass matrices and compare them with 2PA in bulk CdTe. We find that the 2PA is strongly dependent on the size of the QDs becoming smaller with decreasing size, even when normalizing to the volume of the dots. We adapt a simple degenerate 2PA model, based on the effective mass approximation, to nondegenerate 2PA, and this model correctly describes the experimental data for 2-photon energies up to  $\sim 1.4E_g$ . This suggests that, once the spectrum for one size of quantum dot is known, the model can be used for predicting the degenerate and nondegenerate 2PA spectra of different sized QDs of the same semiconductor.

©2005 Optical Society of America

**OCIS codes:** (190.0190) Nonlinear optics; (190.4720) Optics nonlinearities of condensed matter.

---

## References and links

1. A. L. Efros and A. L. Efros, "Interband absorption of light in a semiconductor sphere," *Sov. Semicond.* **16**, 772-775 (1982).
2. L. A. Padilha, A. A. R. Neves, C.L. Cesar, L. C. Barbosa, and C. H. B. Cruz, "Recombination processes in CdTe quantum-dot-doped glasses," *Appl. Phys. Lett.* **85**, 3256-3258 (2004).
3. G. P. Banfi, V. Degiorgio, and D. Ricard, "Nonlinear optical properties of semiconductor nanocrystals," *Adv. Phys.* **47**, 447-510 (1998).
4. I. Gerdova and A Hache, "Third-order non-linear spectroscopy of CdSe and CdSe/ZnS core shell quantum dots," *Opt. Commun.* **246**, 205-212 (2005).
5. D. Cotter, M. G. Burt, R. J. Manning, "Below-band-gap third-order optical nonlinearity of nanometer-size semiconductor crystallites," *Phys. Rev. Lett.* **68**, 1200-1203 (1992).
6. J. T. Seo, Q. Yang, S. Creekmore, D. Temple, L. Qu, W. Yu, A. Wang, X. Peng, A. Mott, M. Namkung, S. S. Jung, J. H. Kim, "Evaluation of nonlinear optical properties of cadmium chalcogenide nanomaterials," *Phys. E* **17**, 101-103 (2003).
7. A. S. Duarte, H. L. Fragnito, and E. Palange, "Light induced permanent modifications of the nonlinear optical properties of semiconductor doped glasses," *Solid State Commun.* **100**, 463-466 (1996).
8. M. Sheik-Bahae, D.C. Hutchings, D. J. Hagan, and E. W. Van Stryland, "Dispersion of bound electron nonlinear refraction in solids," *IEEE J. Quantum Electron.* **27**, 1296-1309 (1991).
9. K. I. Kang, B. P. McGinnis, Sandalphon, Y. Z. Hu, S. W. Koch, N. Peyghambarian, A. Mysyrowicz, L. C. Liu, and H. Risbud, "Confinement-induced valence-band mixing in CdS quantum dots observed by two-photon spectroscopy," *Phys. Rev. B* **45**, 3465-3468 (1992).
10. A. V. Fedorov, A. V. Baranv, and K. Inoue, "Two-photon transitions in systems with semiconductor quantum dots," *Phys. Rev. B* **54**, 8627-8632 (1996).
11. D.C. Hutchings and E. W. Van Stryland, "Nondegenerate two-photon absorption in zinc blende semiconductors," *J. Opt. Soc. Am. B* **9**, 2065-2074 (1992).
12. L.C. Barbosa, V.C.S. Reynoso, A.M. de Paula, C.R.M. de Oliveira, O.L. Alves, A.F. Craievich, R.E. Marotti, C.H. Brito-Cruz, and C.L. Cesar, "CdTe quantum dots by melt heat treatment in borosilicate glasses," *J. Non-Cryst. Solids* **219**, 205-211 (1997).

13. N.F. Borrelli, D.W. Hall, H.J. Holland, and D.W. Smith, "Quantum confinement effects of semiconducting microcrystallites in glass," *J. Appl. Phys.* **61**, 5399-5409 (1987).
14. J. A. Medeiros Neto, L. C. Barbosa, C. L. Cesar, O. L. Alves, and F. Galembeck, "Quantum size effects on CdTeS<sub>1-x</sub> semiconductor doped glass," *Appl. Phys. Lett.* **59**, 2715-2717 (1991).
15. M. Sheik-Bahae, A. A. Said, T. H. Wei, D. J. Hagan, and E. W. Van Stryland, "Sensitive measurement of optical nonlinearities using a single beam," *IEEE J. Quantum Electron.* **26**, 760-769 (1990).
16. R. A. Negres, J. M. Hales, A. Kobayakov, D. J. Hagan, and E. W. Van Stryland, "Experiment and analysis of two-photon absorption spectroscopy using a white-light continuum probe," *IEEE J. Quantum Electron.* **38**, 1205-1216 (2002).
17. P.C. Sercel and K.J. Vahala, "Analytical formalism for determining quantum-wire and quantum-dot band-structure in the multiband envelop-function approximation," *Phys. Rev. B* **42**, 3690-3710 (1990).
18. C. R. M. de Oliveira, A. M. de Paula, F. O. Plentz Filho, J. A. Medeiros Neto, L. C. Barbosa, O. L. Alves, E. A. Menezes, J. M. M. Rios, H. L. Fragnito, C. H. B. Cruz, and C. L. Cesar, "Probing of the quantum dot size distribution in CdTe-doped-glasses by photoluminescence excitation spectroscopy," *Appl. Phys. Lett.* **66**, 439-441 (1995).
19. E. W. Van Stryland, M. A. Woodall, H. Vanherzeele, and M. J. Soileau, "Energy band-gap dependence of 2-photon absorption," *Opt. Lett.* **10**, 490-492 (1985).

## 1. Introduction

The linear and nonlinear optical properties of semiconductor quantum dots (QDs) have been intensely studied in the last decade due to their three-dimensional quantum confinement which gives them interesting properties. The linear properties are quite well understood.[1,2] The electronic density of states changes from the continuum for bulk semiconductors toward a system of discrete states in QDs [1], and the photoexcited carrier recombination time goes from nanoseconds in bulk semiconductors down to picoseconds in QDs due to the high concentration of surface states [2]. Nevertheless, the magnitude and frequency dependence of the nonlinear refractive index,  $n_2$ , and the two-photon absorption coefficient,  $\beta$ , are less well understood. Some authors have experimentally determined that QDs exhibit  $n_2$  and  $\beta$  with the same order of magnitude and similar dispersion to those of bulk materials [3,4], however other authors have reported results for  $n_2$  and  $\beta$  which differ significantly from those predicted by theories for the bulk [5,6]. Additionally, Duarte et. al. [7] has shown that these nonlinear properties can be changed due to a photodarkening effect produced by exposure of the QDs to high laser irradiance. The photodarkening is accompanied by an increase in  $\beta$  and change in value of  $n_2$  along with its possible sign change.[7] A complete understanding of the linear and nonlinear optical properties of semiconductor QDs is desirable, since it would help determine their suitability for possible applications.

In this paper we report measurements of the frequency degenerate and nondegenerate two-photon absorption (2PA) spectrum for different samples of CdTe quantum dots in glass matrices. The experimental results show that these spectra are different from that predicted by the theory for the bulk [8], and strongly depend on the QD size. We propose a theoretical model based on the effective mass approximation for explaining the dependence of spectra on the quantum dot size.

## 2. Theoretical model for nondegenerate 2PA

Theories have already been developed to describe the degenerate 2PA in systems with QDs [9,10]. For direct bandgap semiconductor QDs, Fedorov et. al. [10] proposed a simple theory for both linear absorption and 2PA based on the effective mass approximation. Although this simple model does not consider the band mixing between the light and heavy holes in the valence band [9], it works quite well for describing the linear absorption. Here we extend the theory proposed by Fedorov et. al. [10] to obtain an analytical expression for the nondegenerate 2PA coefficient for semiconductor quantum dots using the well known theory for nondegenerate 2PA in bulk semiconductors [11].

The nondegenerate 2PA transition rate is given by [11].

$$W_{nd}^{(2)} = \frac{2\pi}{\hbar} \sum_{i,f} |M_{f,i}^{nd}|^2 \delta(E_f - E_i - \hbar\omega_2 - \hbar\omega_1), \quad (1)$$

where  $E_i$  and  $E_f$ , represent the energies of the initial and final states [10]. The matrix elements  $M_{f,i}^{nd}$  give the strengths of the transitions between these states:

$$M_{f,i}^{nd} = \sum_a \frac{H_{2f,a} H_{1a,i}}{E_a - E_i - \hbar\omega_1 - i\hbar\gamma} + \frac{H_{1f,a} H_{2a,i}}{E_a - E_i - \hbar\omega_2 - i\hbar\gamma}, \quad (2)$$

where  $a$  represents the intermediate state,  $H_j = (e/mc) \mathbf{A}_j \cdot \mathbf{p}$ ,  $H_{j f,i} = \langle \Psi_f | H_j | \Psi_i \rangle$ , and  $\gamma$  is the inverse of the life-time in each excited state.

For non-centrosymmetric semiconductors, a second channel, which considers the dipole approximation due to the difference in the dipole moment in each band, has to be considered. From Eq. (1) and considering the second channel, the nondegenerate 2PA coefficient is written as:

$$\beta_{ND} = \frac{N\rho}{x_1 x_2^2} \left( \frac{k^2}{E_g^5} \langle F_{ND}^{(2)} \rangle + \frac{Q^2}{E_g^3} \langle \Phi_{ND}^{(2)} \rangle \right), \quad (3)$$

where  $N$  is the QD density in the sample,  $\rho$  is the Maxwell Garnett local field correction,  $E_g$  is the quantum dot bandgap energy,  $x_j = \hbar\omega_j/E_g$ , and  $k$  and  $Q$  are constants which give the strength of each channel. Here,

$$\Phi_{ND}^{(2)} = \sum_{j=1}^3 \sum_i (2l_i + 1) \delta(E_i^c - E_i^{h_j} - \hbar\omega_1 - \hbar\omega_2), \quad (4)$$

describes the transitions due to the difference in the dipole moment, and

$$F_{ND}^{(2)} = \frac{1}{R^2} \sum_{j=1}^3 \sum_{i,f} T_{i,f}^{c,h_j ND} \left( l_f \delta_{l_f, l_i+1} + l_i \delta_{l_f, l_i-1} \right) \frac{\xi_f^2 \xi_i^2}{(\xi_f^2 - \xi_i^2)^2} \delta(E_f^c - E_i^{h_j} - \hbar\omega_1 - \hbar\omega_2), \quad (5)$$

results from Eq. (1). The term  $T_{i,f}^{c,h_j ND}$  is given by,

$$T_{i,f}^{c,h_j ND} = \left| \frac{1}{m^c} \frac{E_g}{E_i^c - E_f^c + \hbar\omega_1 - i\hbar\gamma} + \frac{1}{m^c} \frac{E_g}{E_i^c - E_f^c + \hbar\omega_2 - i\hbar\gamma} + \frac{1}{m^{h_j}} \frac{E_g}{E_i^{h_j} - E_f^{h_j} + \hbar\omega_1 + i\hbar\gamma} + \frac{1}{m^{h_j}} \frac{E_g}{E_i^{h_j} - E_f^{h_j} + \hbar\omega_2 + i\hbar\gamma} \right|^2, \quad (6)$$

$\xi_i$  and  $\xi_f$  are the arguments at which the spherical Bessel functions equal zero, which correspond to the initial and final states respectively [10],  $\langle F_{ND}^{(2)} \rangle = \int_0^\infty f(r) F_{ND}^{(2)} dr$ ,

$\langle \Phi_{ND}^{(2)} \rangle = \int_0^\infty f(r) \Phi_{ND}^{(2)} dr$ , and  $f(r)$  are functions which describe the size distribution of the quantum dots. Usually we can consider  $f(r)$  as a Gaussian distribution. In Eqs. (4) and (5), the

sum over  $j$  means the sum over the three sub-bands in the valence band: heavy holes, light holes, and split-off band [10].

The constants  $k$  and  $Q$  depend only on the semiconductor properties and should be the same for fitting the nondegenerate 2PA spectrum of samples with different size QDs and for different pump photon energies.

### 3. Experimental results

Figure 1 shows the linear absorption spectra for the samples investigated. The details of the glass sample preparation processes are described in Ref. [12,13]. The QD's size and the fill fraction may be estimated by analyzing TEM (Transmission Electron Microscopy) images of the samples.[14] The fill fraction is defined as the fraction of volume of the glass composite material occupied by the quantum dot. Based on TEM imaging, sample CdTe-750 has quantum dots with an average radius of  $6.6 \pm 0.9$  nm, with a QD fill fraction of  $\sim 0.85 \pm 0.17\%$ . The second sample, CdTe-600, has smaller nanoparticles,  $3.2 \pm 0.4$  nm in radius, and a fill fraction of  $\sim 2.0 \pm 0.4\%$ . The third sample, CdTe-570, contains quantum dots with a  $2.9 \pm 0.5$  nm radius, and a fill fraction of  $\sim 1.3 \pm 0.3\%$ . From the linear absorption spectra we find that the bandgap of CdTe-750 is 1.67 eV, of CdTe-600 is 2.07 eV and of CdTe-570 is 2.17 eV, which from the theory correspond to radii of  $6.4 \pm 0.9$  nm for CdTe-750,  $3.1 \pm 0.3$  nm for CdTe-600, and  $2.8 \pm 0.4$  nm for CdTe-570. These values agree closely with the TEM analysis. These analyses show that all the samples have the same structure within the same glass matrix, differing only in the QD size and fill fraction. Because the fill fraction is in the order of  $10^{-2}$ , the relative distance between two QDs is large enough to avoid interaction between QDs.

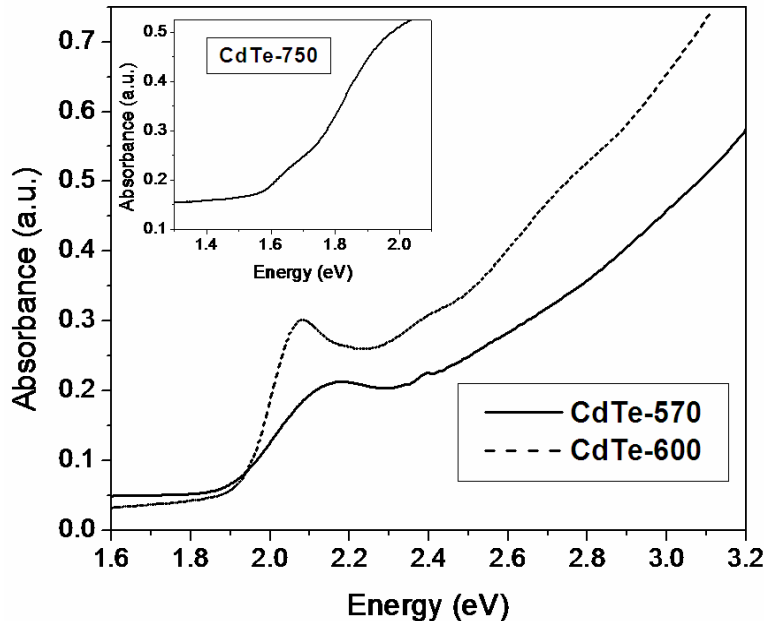


Fig. 1. Linear absorption spectra for CdTe-600 and CdTe-570. The linear absorption for CdTe-750 is shown in the inset.

The degenerate 2PA spectra were measured using open aperture Z-scans [15] at different wavelengths from an optical parametric generator/amplifier (OPA) tunable from 500nm up to 2200nm, that is pumped by a Ti:Sapphire regenerative amplifier with pulses of  $\sim 140$  fs FWHM, at 775nm with a 1 KHz repetition rate. The nondegenerate 2PA spectra were measured by using a femtosecond pump and white-light continuum (WLC) probe [16]. The experimental setup has been previously described in detail [16]. The pump beam is from an

optical parametric generator/amplifier (OPA) identical to that one used for the Z-scan experiment so that we can choose the pump wavelength over a broad spectral range. The probe beam is a femtosecond WLC generated in a CaF<sub>2</sub> crystal pumped by a second OPA set to 1300nm. Spectral filters, with 10nm spectral band, are used for selecting the probe wavelength ( $\lambda_1$ ), so that we are able to study the absorption of the probe photon with energy  $\hbar\omega_1$  due to the presence of the pump photon of energy  $\hbar\omega_2$ . Using filters with different  $\lambda_1$  we can cover the spectrum for the nondegenerate 2PA. The pulsewidths of both pump and probe are independently measured with autocorrelation techniques, and the spatial profiles are also measured [16]. We choose the pump photon energy to be lower than  $E_g/2$ , and we make the probe beam weak enough so that we avoid any degenerate 2PA in these nondegenerate spectral experiments. Although these samples may experience permanent changes in absorption after prolonged illumination at high irradiance, all the data shown in this paper were measured using sufficiently low irradiances to avoid any photoinduced changes in the sample.

Figure 2 shows the degenerate 2PA spectrum and three different nondegenerate 2PA spectra, each one at a different pump photon energy, together with the theoretical curves for CdTe-750, all plotted versus the two-photon energy,  $\hbar\omega_1 + \hbar\omega_2$ , in units of the bandgap energy of the quantum dot. The best fit for all of these spectra is for  $k = 0.135 \pm 0.027$  and  $Q = 0.141 \pm 0.028$ , in Eq. (3).

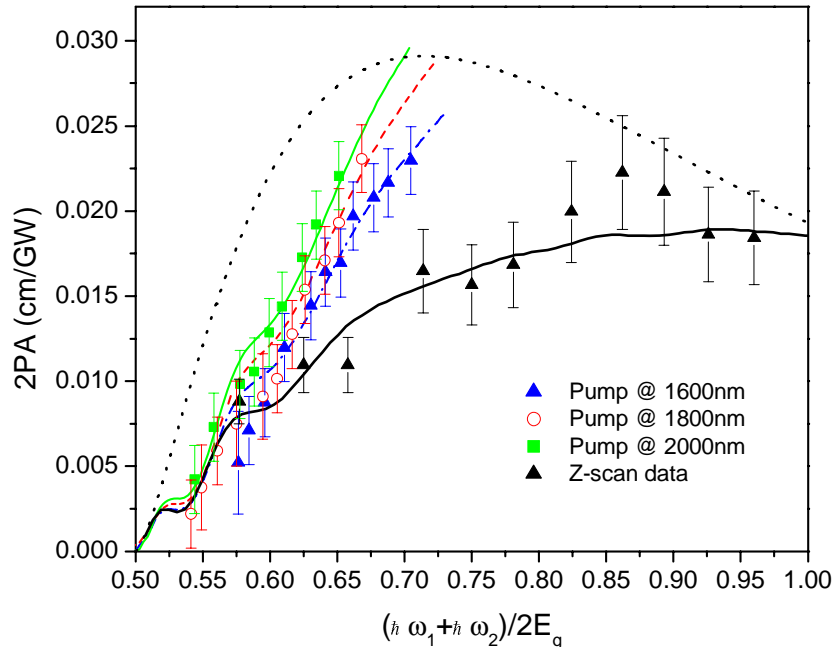


Fig. 2. Degenerate and nondegenerate 2PA spectra for CdTe-750 for three different pump photon energies. For the degenerate Z-scan data  $\omega_1 = \omega_2$ . The lines following the experimental data are calculated from theory, and the dotted line is the theory for degenerate 2PA in bulk CdTe.

Figure 3 is the same as Fig. 2 but for CdTe-600. In this case, the best fitting for this higher QD fill fraction sample uses  $k = 0.124 \pm 0.024$  and  $Q = 0.13 \pm 0.025$ . For the nondegenerate measurements with a pump photon at 1300nm for CdTe-600, the signal is so small that the competing effect of cross phase modulation masks the signal so that we were only able to determine an upper bound on the signal. This is indicated by the large error bars starting from zero in Fig. 3. The values used for  $k$  and  $Q$  in both samples are very similar, the discrepancy of around 10% can be explained mainly by the uncertainty in the QD fill fraction in each

sample which is around  $\pm 20\%$ . Also in Fig. 3 we see that the experimental data for the degenerate 2PA is higher than that predicted by theory, and we do not observe the dip predicted at  $\sim 0.75E_g$ . There are two clear possibilities to explain these discrepancies. First, this theory does not consider the band mixing between the heavy and light hole bands, which has been observed in QDs [9, 17, 18]. Such band mixing can allow transitions at wavelengths that would eliminate the dip seen in Fig. 2. The simpler theory also presents some dips when it is used to fit the linear absorption spectrum, and those dips are eliminated by considering the theory proposed in Ref. [17,18] The second reason can be from the effects of photodarkening which occurs in QD doped glass matrices when they are exposed to high intensity laser light as in a Z-scan experiment [7].

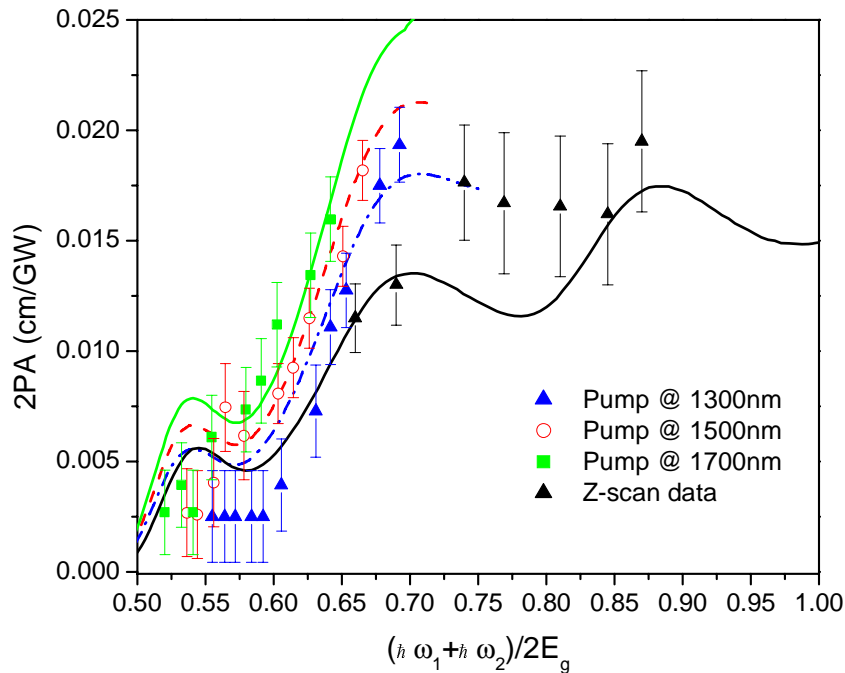


Fig. 3. Degenerate and nondegenerate 2PA spectra for CdTe-600 for three different pump photon energies. For the degenerate Z-scan data  $\omega_1 = \omega_2$ . The lines following the experimental data are calculated from theory.

In Fig. 2 we compare the degenerate 2PA spectrum for CdTe-750 with the curve predicted for the bulk [19]. While the bulk theory shows a peak near  $0.7 E_g$ , the nondegenerate data is nearly monotonically increasing up to very near  $E_g$ . Figures 2 and 3 show that for the same two-photon energy the nondegenerate 2PA coefficient is higher for higher  $h\omega_i$ , and the nondegenerate 2PA is also higher than that for the degenerate case. The enhancement of the nondegenerate 2PA coefficient as the probe photon energy goes closer to the linear absorption edge is predicted by the theory and it indicates that, as in bulk semiconductors, for the same two-photon energy it is more probable to absorb two photons with different energies than two photons with the same energy. This occurs because in the nondegenerate case, one of the photons has an energy closer to  $E_g$  and hence is closer to the intermediate state resonance.

In Fig. 4 we compare the spectra for the different size quantum dots. Here we normalize the 2PA coefficients by dividing by the fill fraction and by the Maxwell-Garnet local field penetration, which is a factor 0.30 for each sample. We observe that the nondegenerate 2PA coefficients are size dependent. From comparisons of Figs. 2 and 3 we also see that the degenerate  $\beta$ 's are different. The theoretical curves in Fig. 4 show in addition that the first peak in the 2PA is blue shifted as the quantum dot size is decreased, and the 2PA coefficient is reduced for smaller QDs. The 2PA coefficient depends on the density of possible transitions

and this density is proportional to  $R^2$ . For smaller quantum dots, the number of possible transitions per unit energy is lower and, consequently the probability for 2PA is decreased. Also, the quantum confinement introduces an increase in the bandgap energy, which from Eq. 3 gives a decrease in the 2PA coefficient. For CdTe-570 all the measurements showed a nondegenerate 2PA coefficient with at least 100% error due to our experimental sensitivity of  $\sim 0.6\%$  of the normalized transmittance measured. Based on the fitting of the two larger QD samples, we use  $k = 0.129$  and  $Q = 0.135$  to estimate the nondegenerate 2PA coefficient for CdTe-570. The theoretical value for this sample presents a maximum value of  $\sim 0.002$  cm/GW, which is consistent with our experimental result.

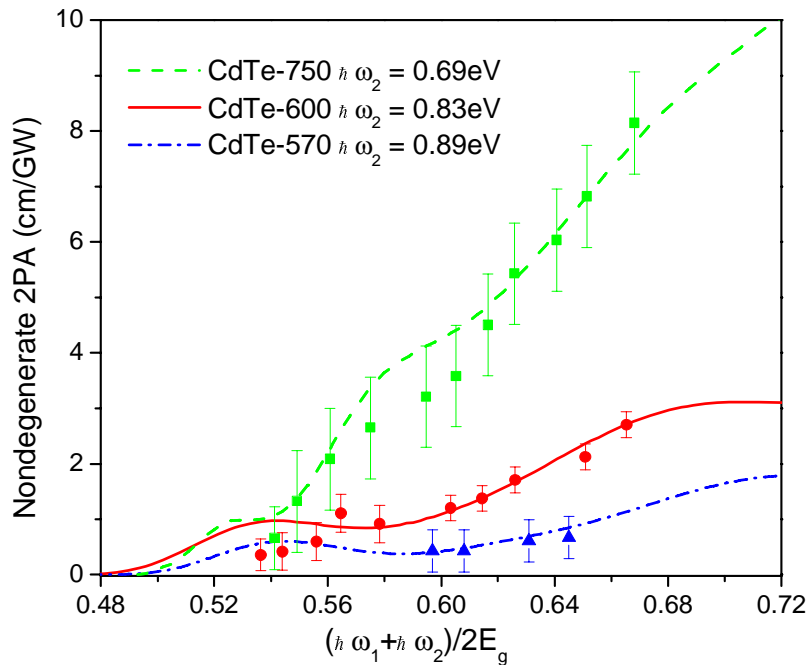


Fig. 4. Comparison of the nondegenerate 2PA spectra for the three different samples normalized by the fill fraction of each sample and by the Maxwell-Garnet local field correction

#### 4. Conclusion

In conclusion, the experimental results have shown that both the degenerate and nondegenerate 2PA spectra in systems with semiconductor QDs are different from that for bulk semiconductors and are strongly size dependent. For smaller QDs the experimental data showed lower 2PA coefficients and those values decrease faster than for larger QDs as the wavelength approaches the 2PA edge. The proposed theory for the nondegenerate case is based on a simple model; nevertheless, it fits the entire set of data for the samples studied. The close agreement between fitted values for material constants  $k$  and  $Q$  used in the theory for the spectra of CdTe-600 and CdTe-750 suggests that the proposed model can be used for predicting the degenerate and nondegenerate 2PA spectra of different sized QDs of the same semiconductor. Once the values for  $k$  and  $Q$  are determined for the degenerate spectrum, this theory can also predict the values of the nondegenerate spectra and vice-versa. The close agreement between theory and experiment indicates that contributions of surface states to the 2PA is negligible in these samples.

## **Acknowledgments**

The authors acknowledge Prof. Anatoly Fedorov for his helpful discussions. LA Padilha thanks CAPES and FAPESP for financial support. We also gratefully acknowledge the support of the National Science Foundation ECS 0217932, the US Army Research Laboratory, and the Naval Air Warfare Center Joint Service Agile Program (contract number N00421-04-20001).